Temporal Control over Transient Chemical Systems using Structurally Diverse Chemical Fuels

(Article begins on next page)

Temporal Control over Transient Chemical Systems using Structurally Diverse Chemical Fuels

Jack L.-Y. Chen,[b] Subhabrata Maiti,[a] Ilaria Fortunati,[a] Camilla Ferrante,[a] and Leonard J. Prins*[a]

Abstract: The next generation of adaptive, intelligent chemical systems will rely on a continuous supply of energy to maintain the functional state. Such systems will require chemical methodology that provides precise control over the energy dissipation process, and thus, the lifetime of the transiently activated function. Herein we show the use of structurally diverse chemical fuels to control the lifetime of two different systems under dissipative conditions: transient signal generation and the transient formation of self-assembled aggregates. The energy stored in the fuels is dissipated at different rates by an enzyme, which installs a dependence of the lifetime of the active system on the chemical structure of the fuel. In the case of transient signal generation, it is shown that different chemical fuels can be used to generate a vast range of signal profiles, allowing temporal control over two orders of magnitude. Regarding self-assembly under dissipative conditions, the ability to control the lifetime using different fuels turns out to be particularly important as stable aggregates are formed only at well-defined surfactant/fuel ratios, meaning that temporal control cannot be achieved by simply changing the fuel concentration.

Introduction

Nature has long been an inspiration for chemists interested in the design of molecular receptors, catalysts, and materials.[1] Over the past decades this has led to the generation of a wealth of synthetic systems able to mimic basic natural functions, whilst integrating also non-natural elements and operating also in non-physiological conditions. And yet the leap towards synthetic systems that display advanced biological functions, such as the ability to communicate, grow, adapt and even evolve is still a very large one.[1b] One aspect currently receiving a great deal of attention is the development of synthetic systems that require energy to be functional (Figure 1).[1a,b,2] Such systems reside in an unproductive, native resting state and energy input is required for activation and for expression of the associated functions. Energy dissipation—through physical or chemical pathways—then leads to a spontaneous return to the inactive state.[3] Several recent examples of chemical systems that employ energy for the contro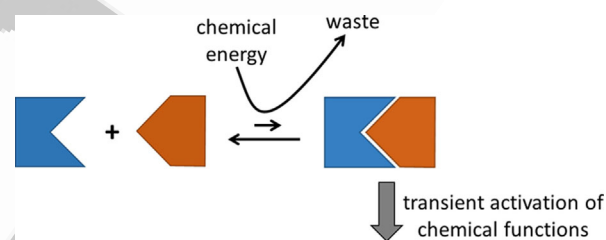lled self-assembly of functional structures have been reported,[4,5] though much fewer systems are able to spontaneously dissipate the added energy.[6] The exciting initial reports of systems operating akin to living ones shed light on their enormous potential in the fields of materials science,[7] nanotechnology,[2f,8] catalysis, and medicine.[5b,9]

Nature itself uses predominantly the chemical energy stored in high-energy molecules such as adenosine triphosphate (ATP) or guanosine triphosphate (GTP)■■definitions ok?■■ for the transient activation of biological processes.[10] Early examples of systems triggered by the addition of high-energy molecules involve synthetic systems coupled to natural dissipative systems[11] or coupled to chemical oscillators.[12] Although functional, these systems can be difficult to modulate and thus there is a need for synthetic systems with greater flexibility.[13] Recently, examples of synthetic, dissipative processes driven by a chemical fuel have been developed for the transient formation of physical structures, such as gels,[14] vesicles,[15] and molecular cages,[16] but also for the regulation of chemical processes, such as signal generation[17] and catalysis.[16b]

Figure 1. Schematic representation of a system that requires a chemical fuel for activation and expression of its associated functions.

[a] Dr. S. Maiti, Dr. I. Fortunati, Prof. Dr. C. Ferrante, Prof. Dr. L. J. Prins
Department of Chemical Sciences
University of Padova
Via Marzolo 1, 35131 Padova (Italy)
E-mail: leonard.prins@unipd.it

[b] Dr. J. L.-Y. Chen
School of Science
Auckland University of Technology
34 St Paul St, Auckland 1010 (New Zealand)

The ORCID identification number(s) for the author(s) of this article can be found under https://doi.org/10.1002/chem.201701533.

To gain further advances in this field however, we need to exploit the inherent advantages of dissipative systems. The ability to dissipate energy gives a system the possibility to return to the basal resting state and the capacity to respond to another stimulus. What if the same system receives a different stimulus? The ability of systems to react differently to diverse stimuli will allow for the construction of systems that are truly adaptive and life-like. Towards this goal, we first need strategies that possess a large degree of flexibility in terms of building blocks, chemical fuels, and associated functions. Herein we provide examples of synthetic systems that are able to respond differently to a range of structurally diverse chemical fuels. It is shown that this provides an excellent way to gain precise temporal control over the chemical functions associated with the system, which is not possible for systems at thermodynamic equilibrium or kinetically trapped in a metastable state. In the longer term, one can envision that such transient systems will eventually allow the development of complex chemical networks[18] which are able to communicate and adapt through an exchange of energy.[1b, 2c] The flexibility of the current methodology is demonstrated by showing that the same approach can be used to regulate entirely different processes, those of signal generation and self-assembly.

Results and Discussion

Transient signal generation

Cells and organelles in nature use small molecules for communication.[19] Neurons for example, release neurotransmitters into the synaptic cleft that triggers a signal response in the postsynaptic neuron. This signal, however, is short-lived. The neurotransmitter is quickly degraded and the signal disappears. The system returns to its basal resting state so that it can be re-used and re-activated. The vast majority of supramolecular systems that have been used to produce a 'signal' rely on the attainment of an activated 'steady state' (Figure 2a).[20] Here, with the system being at thermodynamic
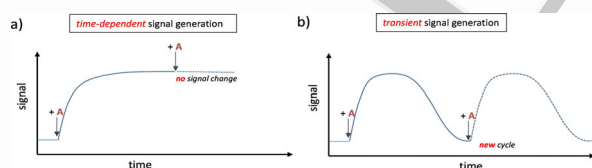

Figure 2. a) Time-dependent signal generation vs. b) transient signal generation. The symbol **A** indicates the arrival of trigger to the system.

equilibrium, the signal persists in time. Although this is a desired situation for many applications, particularly in diagnostics, it does not permit transient signal generation as used by nature. In order to develop systems for transient signal generation, a mechanism must exists that causes the spontaneous disappearance of the signal and a return of the system to the initial resting state, which can then be re-activated upon the arrival of a new trigger (Figure 2b).

Recently, we reported a supramolecular system that uses ATP as a chemical fuel to trigger the generation of signals that are transient in nature.[17] It centres on gold nanoparticles (Au NP **1**) that are covered with a monolayer of thiols terminating with positively charged triazacyclononane·Zn^{2+} (TACN·Zn^{2+}) groups (Figure 3a).[21] The surface of the monolayer is thus highly positively charged and can attract oligoanions which are present in the solution (aqueous buffer).[22] The 'signal' in this system is given by negatively charged fluorescent probes, which are bound to the surface of the positively charged gold nanoparticles in the resting state, in which the fluorescence of the molecules is quenched by its proximity to the gold core (Figure 3b).[23] The addition of highly-charged ATP results in the displacement of the fluorescent probes and the generation of a fluorescent signal. The high affinity of ATP originates from its ability to establish multiple, electrostatic interactions between its phosphate groups and the TACN·Zn^{2+} complexes on the surface of the Au nanoparticles. Establishing the same number of electrostatic interactions with singly charged anions is much more unfavourable from an entropic point of view. Indeed, displacement studies demonstrated that ATP had roughly 3×10^3 times higher affinity for the surface compared to a mixture of AMP + 2P$_i$ with the same number of negative charges.[17] Thus, ATP is a high energy molecule, where entropic cost was paid during its synthesis. This chemical energy, however, can be released by the enzyme-mediated hydrolysis of ATP into AMP + 2P$_i$, which allows a return of the system to the initial resting state with the fluorescent probe bound to the Au NPs. Thus, under the dissipative conditions installed by the presence of the enzyme, ATP acts as a chemical fuel able to transiently dislocate the fluorescent probe from the surface. This system was exciting as it represented one of the first examples of transient signal generation in a supramolecular system driven by molecules. It allowed the mimicking of several key features of natural signalling pathways such as control over output signal intensity and signal duration through regulation of the fuel-level and the rate of energy dissipation.

Nature, however, employs numerous different triggers to elicit a variety of responses. For example, the purinergic signaling pathway is involved in the regulation of various physiological functions in the circulatory, immune and nervous systems, amongst others.[24] It operates through the activation of membrane-bound purinergic receptors by extracellular nucleotides and nucleosides. It is known that receptors belonging to the P2Y family are stimulated by a variety of nucleotides, such as ATP, ADP and UTP. In order to exploit the full potential of synthetic dissipative systems, they need also to respond to different chemical triggers, and preferably with unique responses. Our system described above could utilise only ATP as a chemical fuel due to the substrate specificity of the employed enzyme potato apyrase.[25] To expand the scope, our synthetic system must be able to respond to more than a single chemical fuel. Towards this goal, we began to investigate different enzymes which could be compatible with our system. We were immediately drawn to phosphatases,[26] which are enzymes that cleave the phosphate group from phosphorylated compounds. Our interest in phosphorylated compounds came
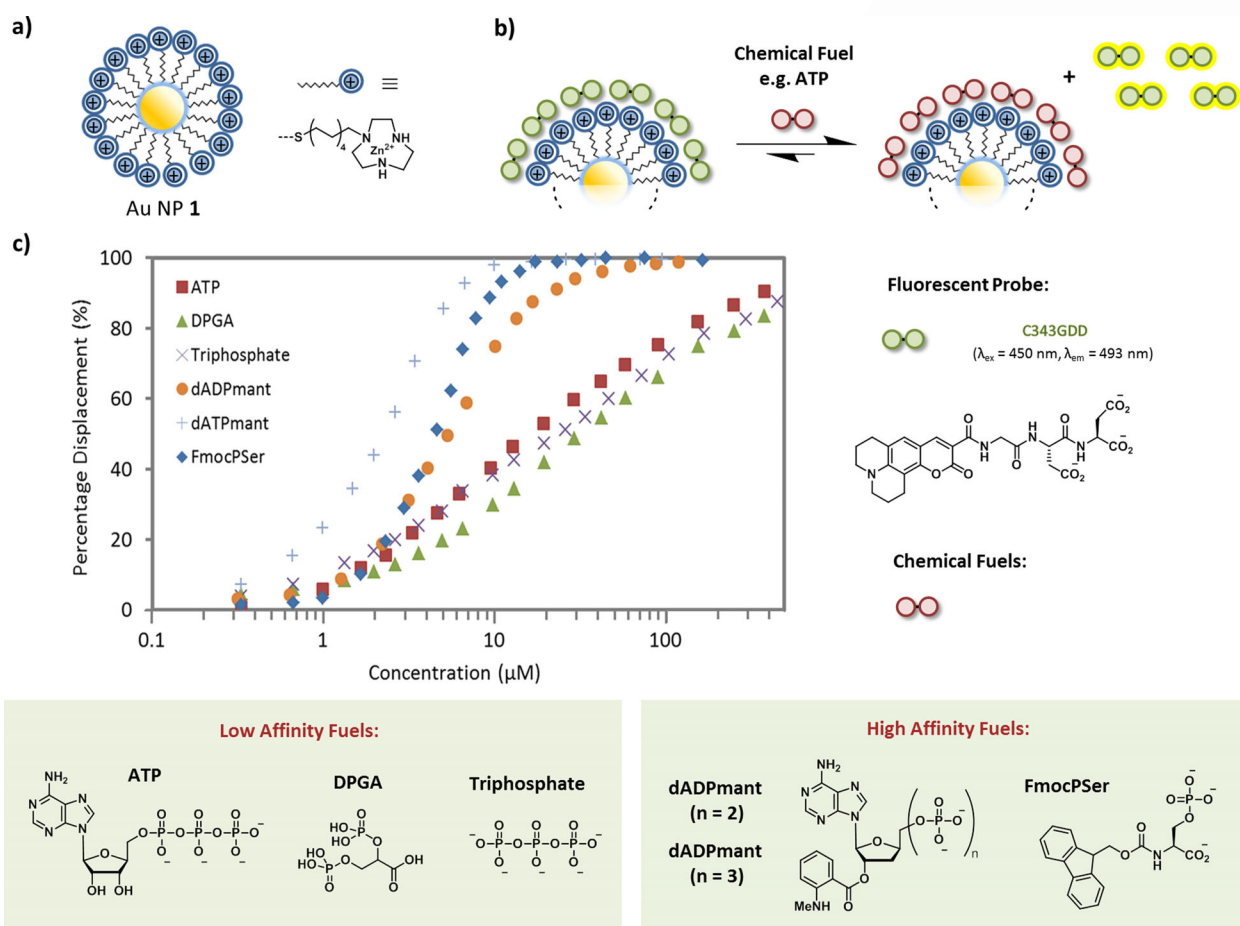
↖↖ These are not the final page numbers!

Figure 3. a) Schematic representation of the gold nanoparticles (Au NP **1**) used in the system. b) Schematic showing the displacement of fluorescent probe C343GDD from the surface of Au NP **1** upon the addition of a competitor. c) Percentage displacement of C343GDD as a function of the concentration of different phosphorylated molecules. Experimental conditions: [TACN] = 10 μM ± 1 μM, [C343GDD] = 3.0 μM, [HEPES] = 10 mM, pH 7.0, [Zn(NO$_3$)$_2$] = 100 μM, [MgCl$_2$] = 5 mM, T = 37 °C, λ_{ex} = 450 nm, λ_{em} = 493 nm, slits = 2.5/5.0 nm, the average error in these measurements is 5%.

from our previous observations that, in particular, this class of molecules (compared to, for example carboxylate-containing compounds) have enhanced affinity for the surface of Au nanoparticles that are covered with TACN·Zn^{2+} headgroups.[27] Ultimately, we chose alkaline phosphatase,[28] a readily available enzyme with broad substrate scope, which would allow us to employ numerous phosphorylated compounds as chemical fuels. We reasoned that different chemical fuels could be found that would interact differently with the nanoparticle surface (different affinities) and that temporal control of energy dissipation rates could be governed by the substrate preference of the enzyme alkaline phosphatase. This would allow us to control both the intensity and duration of a generated signal by careful selection of the chemical trigger.

We began by investigating the affinity of several structurally diverse phosphorylated molecules for Au NP **1**. This was achieved by monitoring the displacement of the fluorescent probe C343GDD (3.0 μM) from the monolayer surface upon the addition of each of the phosphorylated molecules at increasing concentrations (Figure 3 c). The compounds tested included phosphorylated carbohydrates, phosphorylated amino acids and nucleoside phosphates. Of all the compounds tested, di-

phosphoglyceric acid (DPGA) had the lowest affinity for the nanoparticle surface, displacing only 30% of the fluorescent probe at a concentration of 10 μM. Of slightly higher, but nearly identical, affinity for the Au NP surface were ATP and inorganic triphosphate and therefore these three compounds were grouped together as the 'low affinity' chemical fuels. Other molecules were found which possessed significantly stronger affinity for Au NP **1**, which included dADP$_{MANT}$, dATP$_{MANT}$ and the phosphophorylated amino acid Fmoc-phosphoserine (FmocPSer). The significantly higher binding affinity of this group of molecules can be ascribed to strong hydrophobic contributions from the aromatic 'mant' (methylanthraniloyl) and Fmoc-groups that complement the electrostatic interactions. These hydrophobic interactions have been previously observed to significantly increase the affinity of oligoanions for the surface of these monolayer covered nanoparticles.[22a] This second group of three molecules all displaced > 70% of the fluorescent probe at a concentration of 10 μM, and were grouped together as the 'high affinity' chemical fuels (FmocPSer, dADP$_{MANT}$ and dATP$_{MANT}$).

Experiments were next set up to investigate transient signal generation by these chemical fuels under dissipative condi-
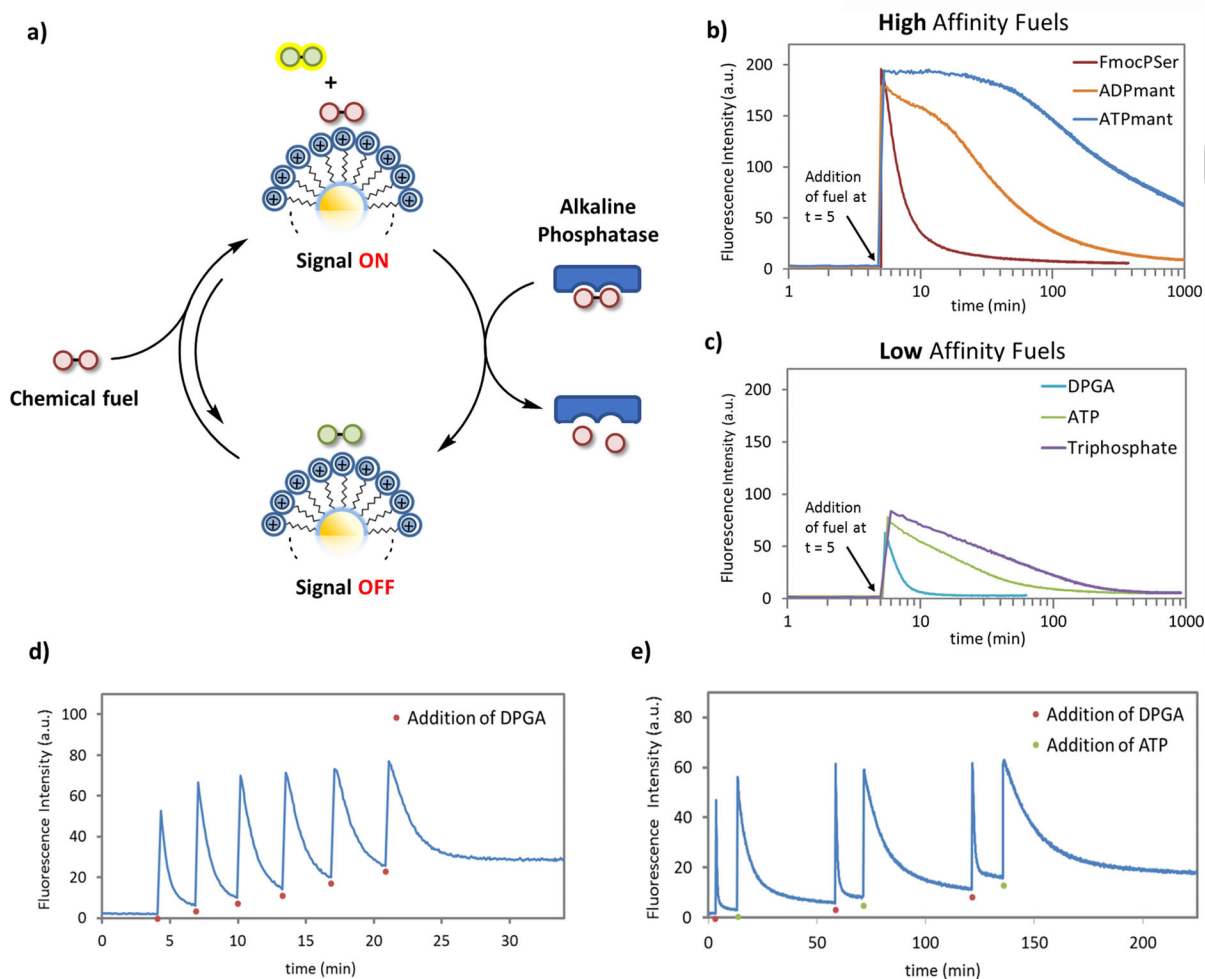
Figure 4. a) Schematic representation of the system for dissipative signal generation. b) Fluorescence intensity at 493 nm as a function of time upon the addition of 'high affinity' chemical triggers and c) 'low affinity' chemical triggers. Experimental conditions for b) and c): [TACN] = 10 ± 1 μM, [C343GDD] = 3.0 μM, [HEPES] = 10 mM, pH 7.0, [Zn(NO₃)₂] = 100 μM, [MgCl₂] = 5 mM, [alkaline phosphatase] = 1 U m⁻, [chemical fuel] = 10 μM, T = 37 °C, λ_{ex} = 450 nm, λ_{em} = 493 nm, slits = 2.5/5.0 nm. d) Fluorescence intensity at 493 nm upon 6 repetitive additions of DPGA. Experimental conditions: [TACN] = 10 ± 1 μM, [C343GDD] = 3.0 μM, [HEPES] = 10 mM, pH 7.0, [Zn(NO₃)₂] = 100 μM, [MgCl₂] = 5 mM, [alkaline phosphatase] = 3 U m⁻, [DPGA] = 10 μM (×6), T = 37 °C, λ_{ex} = 450 nm, λ_{em} = 493 nm, slits = 2.5/5.0 nm. e) Fluorescence intensity at 493 nm following sequential additions of DPGA and ATP. Experimental conditions: [TACN] = 10 ± 1 μM, [C343GDD] = 3.0 μM, [HEPES] = 10 mM, pH 7.0, [Zn(NO₃)₂] = 100 μM, [MgCl₂] = 5 mM, [alkaline phosphatase] = 5 U m⁻, [DPGA] = 10 μM (×3), [ATP] = 8 μM (×3), T = 37 °C, λ_{ex} = 450 nm, λ_{em} = 493 nm, slits = 2.5/5.0 nm.

tions, that is, in the presence of the enzyme alkaline phosphatase. Each fuel (10 μM) was added to a buffered solution pre-equilibrated with Au NP **1** ([TACN·Zn²⁺] = 10 μM), the fluorescent probe C343GDD (3 μM) and the enzyme alkaline phosphatase (1 U m⁻). Addition of a specific fuel triggered the immediate appearance of a fluorescent signal due to the displacement of C343GDD from the surface of the Au NPs (Figure 4a). This signal gradually disappeared as the alkaline phosphatase hydrolysed the chemical fuel to form the dephosphorylated, low affinity products. The decay rate for the signal generated by each compound was dependent on a combination of the enzyme's substrate-dependent hydrolysis rate, and the degree of phosphorylation of the compound employed. From the 'high affinity' group of chemical triggers, FmocPSer was hydrolysed the most rapidly by alkaline phosphatase, with a signal decrease of 50 % after just 1.7 min (Figure 4b). Addition of the same amount of dADP$_{MANT}$ generated an initial signal of similar intensity, but this signal was dissipated 17 times slower, requir-

ing 28 min for a 50 % reduction of the signal. Likewise, the use of the same amount of dATP$_{MANT}$ as a trigger resulted in an almost identical signal intensity, but this time the duration of the induced signal was longer still, by a further factor of 11 ($t_{50\%}$ = 300 min). Thus, by simply changing the chemical fuel used to activate the system, temporal control of the generated signal is readily achieved, with the duration of the induced signal able to span more than two orders of magnitude ($t_{50\%,ATPMANT}$: $t_{50\%, FmocPSer}$ = 176, note the logarithmic scale in Figure 4b).

A similar effect could also be achieved with the series of 'low affinity' binders (Figure 4c). These three chemical triggers, DPGA, ATP and triphosphate all bind Au NP **1** more weakly, causing partial displacement of the fluorescent probes at the same fixed concentration of 10 μM as used before. In this case, the addition of DPGA (10 μM) generates a low intensity signal which very rapidly ($t_{50\%}$ = 1.2 min) disappears by the action of alkaline phosphatase. Alternatively, a signal which lasts 10

↖↖ These are not the final page numbers!

times longer can be generated by the addition of ATP ($t_{50\%}=$ 12.5 min). Triphosphate is a much poorer substrate for alkaline phosphatase, with a hydrolysis rate so slow that the signal lasts for longer than 300 min ($t_{50\%}=$ 33.3 min). Figure 4d shows the possibility to reactivate the system following energy dissipation. DPGA was used because of the speed at which the signal disappears in the presence of alkaline phosphatase. In this experiment, DPGA (10 μм) was used to repeatedly activate the system six times. The baseline can be seen to gradually rise over time due to the build-up of waste (inorganic phosphate) as a by-product of phosphatase activity, slowly reaching concentrations at which it can compete with **A** for binding to Au NP **1**. Interestingly, the same system can also effectively respond to a combination of different chemical triggers. In Figure 4e, the system is shown to be first activated by DPGA (10 μм), which is quickly hydrolysed prior to the addition of a second chemical trigger (ATP, 10 μм) which is slowly depleted. This sequence can be repeated, demonstrating the possibility to effectively control signal duration using chemical fuels.

The above experiments demonstrate that the enzyme alkaline phosphatase provides versatility and robustness to the signal generation process. Six different chemical fuels have been used, each producing a distinctive signal profile in time in terms of intensity and duration when added at the same concentration. Countless other chemical triggers could be easily designed and tailored to give the desired intensity and duration of signal, which makes this system an excellent platform for the generation of more complex systems.

Self-assembly under dissipative conditions

Dissipative systems are found in nature not only for signal generation, but perhaps even more importantly, for the transient formation of physical structures.[5] Notably, nature uses high-energy molecules (such as ATP and GTP) as chemical fuels to drive these processes. Microtubules for example are formed when required (during cell division) and destroyed when they are not.[29] Microtubules are hollow cylinders made up of polymerized α- and β-tubulin dimers. Yet, polymerization of these dimers requires a change in their innate conformation which occurs upon the complexation of GTP. Subsequent to assembly, the GTP bound to β-tubulin is hydrolyzed, dissipating the energy stored in GTP. This pushes the dimer to a strained, high energy state in the polymer leading to spontaneous dissociation at the ends of the microtubules. Thus, in this process, energy dissipation leads to structural instability.

Recently, we have shown that a similar mechanism can be installed in a synthetic system[15a] by demonstrating that ATP can act as a chemical fuel for the transient formation of vesicles (Figure 5).[30] The approach relied on the stabilisation of cationic vesicles through non-covalent interactions between ATP and C16-surfactants terminating with the same TACN·Zn^{2+} -head group as used in the AuNP-based system discussed above (C$_{16}$TACN·Zn^{2+}, Figure 5b). The inspiration for ATP-induced formation of vesicles came from prior reports that the stabilisation of such structures formed from charged surfactant molecules could be promoted by the presence of multiply charged counter ions.[31] Importantly, like in microtubule formation, the in situ hydrolysis of ATP by the enzyme potato apyrase leads to dynamic instability, because the removal of ATP brings the aggregated surfactant molecules into an unstable high-energy state. In the case where a new ATP molecule is present to stabilize the system, the aggregate will persist, otherwise disaggregation of the structure will occur (see Figure 5a). This implies that under dissipative conditions, installed by the presence of the enzyme, a continuous supply of fresh ATP is required to maintain structural stability. It is worth noting though, that a difference exists between this system and microtubule formation. Microtubule formation is an intrinsically dissipative process, because it is the assembly itself which catalyses the hydrolysis of the fuel. Our system, like most, but not all, synthetic systems relies on an external constituent—the enzyme—for energy dissipation.[16b]

Considering the success in regulating transient signal generation with different chemical fuels, we became interested to determine whether different fuels could be used in a similar way to control the transient self-assembly process. In particular, we were interested to determine if different chemical fuels could be employed to control the lifetime of these supramolecular structures. DPGA and triphosphate were chosen as two chemical fuels to compare with the results obtained for vesicle formation with ATP. The nanoparticle studies had shown that, together with ATP, these molecules cover a wide range of life times at the same concentration.

First, the aggregation behaviour of C$_{16}$TACN·Zn^{2+} in the absence of fuels was monitored by the addition of increasing amounts of the surfactant into an aqueous solution buffered at pH 7.0 containing the fluorescent apolar probe 1,6-diphenyl-1,3,5-hexatriene (DPH, $\lambda_{ex}=$ 355 nm, $\lambda_{em}=$ 428 nm). DPH is solubilised by the hydrophobic environment of the aggregates and therefore an increase in fluorescence intensity is observed once the critical aggregation concentration (CAC) is reached (Figure 5c). In the absence of any additives, the CAC value for C$_{16}$TACN·Zn^{2+} was determined to be around 100 μм, a figure which compares well with previous reports.[32] The hydrodynamic diameter of the structures formed at a surfactant concentration of 200 μм was determined using dynamic light scattering (DLS) to be 5.9 ± 1.3 nm, which indicated that the structures formed at concentrations of surfactant above 100 μм were micellar aggregates (Figure 5d).

Next, we wanted to examine if different self-assembled structures could be induced by the presence of the different chemical fuels. Titrations of surfactant C$_{16}$TACN·Zn^{2+} were thus conducted in the presence of 10 μм of the phosphorylated molecules DPGA and triphosphate and compared to the results previously obtained for ATP (Figure 5c). In both cases, the fluorescence intensities of the solutions began to increase at similar concentrations of surfactant as in the case for ATP, giving CAC concentrations around 10 μм. For all the samples involving an added oligoanion, the fluorescence values levelled off at well-defined surfactant concentration before increasing again at 100 μм, following the curve measured in the absence of added oligoanions (Figure 5c). The lowering of the CAC shows the effectiveness of all the added molecules in stabilis-
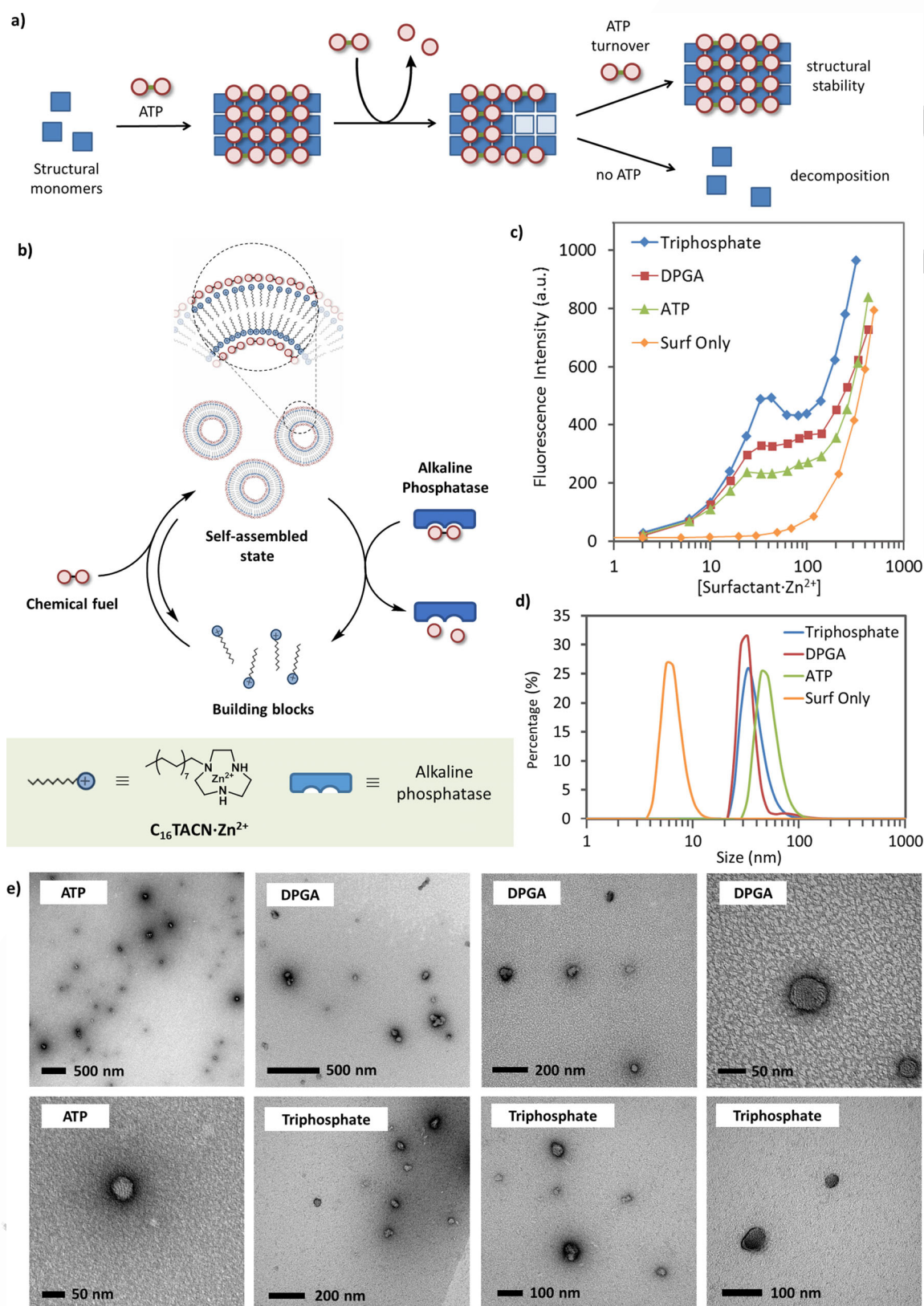
Figure 5. a) Schematic showing the dynamic nature of a dissipative self-assembled system stabilised by a chemical fuel. b) Schematic representation of the dissipative self-assembly of vesicles. c) Fluorescence intensity at 428 nm as a function of the concentration of $C_{16}TACN \cdot Zn^{2+}$ (0–300 μM) added to an aqueous buffer solution containing different concentrations of phosphorylated compounds (10 μM) in the presence of DPH (2.5 μM) as the fluorescent probe. Experimental conditions: [HEPES] = 5 mM, pH 7.0, T = 37 °C, λ_{ex} = 355 nm, λ_{em} = 428, slits = 5/10 nm. d) Hydrodynamic diameter of the aggregates formed from $C_{16}TACN \cdot Zn^{2+}$ (200 μM) in the absence and presence of different phosphorylated compounds (40 μM) measured by DLS in aqueous buffer solution (HEPES, 5 mM, pH 7.0). e) TEM image of vesicles with [$C_{16}TACN \cdot Zn^{2+}$] = 25 μM in HEPES buffer (5 mM, pH 7) with either [ATP] = 5 μM, [DPGA] = 5 μM or [triphosphate] = 5 μM.

↖↖ These are not the final page numbers!

ing the formation of the supramolecular structures. Although globally similar, certain differences exist between the three samples.

The first is the oligoanion/surfactant ratio at which the plateau level is reached (1:2.4, 1:3.3, and 1:4.2, for ATP, DPGA, and triphosphate, respectively), which clearly indicates the different compositions of these aggregates. This also implies that the chemical structure of the fuel determines the amount of aggregates formed at a given fuel concentration. This is confirmed by the observation that the fluorescence intensity at the plateau-level increases as the ratio of fuel/surfactant increases. It is noted that the fluorescence intensity depends on the amount of fluorescent probe DPH that is taken up by the aggregates, that is, the amount of hydrophobic domain generated. The trace with triphosphate shows a peculiar increase in fluorescence intensity, followed by a slight decrease, before increasing sharply again at 100 μM. This suggests that the actual supramolecular structures that are formed may differ at different oligoanion/surfactant ratios. This aspect was further investigated using DLS measurements.

DLS measurements of solutions containing 30 μM of $C_{16}TACN \cdot Zn^{2+}$ and 10 μM of ATP (surfactant/ATP = 3:1) demonstrated the formation of structures with a hydrodynamic diameter of 58 ± 16 nm (Figure 6), which based on a combination of analytical techniques and experiments described earlier, were found to be consistent with a vesicular structure.[15a] This was confirmed by transmission electron microscopy (TEM), in which the formation of vesicle-like spherical aggregates was observed (see Figure 5e). At the same concentration of surfactant (30 μM), but with lower amounts of ATP (2–4 μM, that is, surfactant/ATP ratios of around 10:7), aggregates with similar average sizes of around 40–50 nm were measured (Figure 6), but these values were characterised by poor reproducibility. This was due to the low concentration of aggregates present at these concentrations, which was highlighted also by the large attenuator reading given by the DLS instrument (see experimental section). Good quality DLS data could be obtained
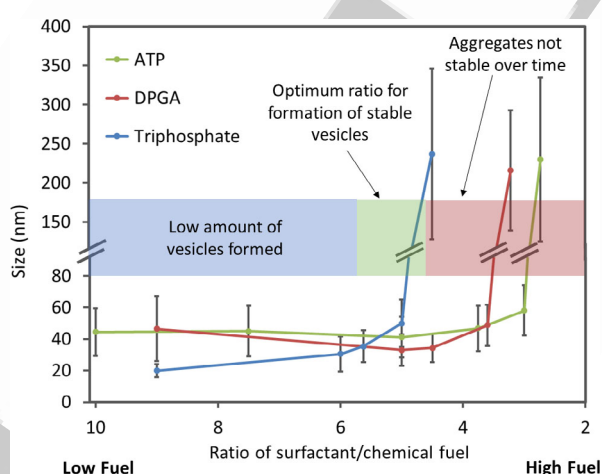

Figure 6. DLS data showing the size of aggregates at different ratios of surfactant to chemical fuel, with error bars showing the standard deviation in nm. Experimental conditions: $[C_{16}TACN \cdot Zn^{2+}] = 30$ μM in 5 mM HEPES (pH 7) and varying concentrations of ATP, DPGA and triphosphate.

once the ATP concentration reached a range of 6–10 μM (ratio = 5:1–3:1). This was characterised by very little variation between replicate readings and low dispersity (< 0.2, see experimental section). The presence of a substantial amount of aggregates was also apparent due to the decrease in the attenuator value given by the DLS instrument at these conditions. The addition of higher amounts of ATP, however, induced the formation of much larger aggregates (surfactant/ATP ratio of 2.7:1 gave an initial size of 230 ± 105 nm). These aggregates continued to increase in size over time, with eventual precipitation of the components out of the solution. With this study, it became obvious that there was an optimum range of surfactant/fuel ratios that allowed the formation of stable vesicles. At too low ratios of surfactant/fuel, the concentration of the added chemical fuel is not yet sufficient to effectively stabilise the formation of vesicles–resulting in a low concentration of aggregates. On the other hand, at high surfactant/fuel concentrations, the uncontrolled formation of larger aggregates is observed. For ATP, this upper limit of surfactant/fuel is around 3 surfactant molecules to 1 ATP molecule as determined by DLS measurements, which is slightly higher than the ratio obtained in the above fluorescence studies (Figure 5c) and is in agreement with earlier work.[15a] These aggregates were found to be stable over prolonged periods of time (10 hours).

The same DLS study was conducted using DPGA and triphosphate to determine the optimal conditions for aggregate formation with these new chemical triggers. First, increasing amounts of the chemical fuel DPGA was added to a fixed concentration of surfactant $C_{16}TACN \cdot Zn^{2+}$ (30 μM) in HEPES pH 7 buffer (5 mM). At low concentrations of DPGA (surfactant/DPGA = 9:1), the size of the particles measured were 46 ± 20 nm though again there was poor reproducibility between measurements. This, combined with the high attenuation value required for the measurement suggested a low concentration of aggregates present. Effective aggregate formation was observed at surfactant/DPGA ratios of around 5:1 down to around 3.5:1, where sizes of 34 ± 9 nm and 48 ± 13 nm were observed, respectively. At surfactant/DPGA ratios lower than 3.5:1, an initial size distribution of 216 ± 77 nm was observed, which steadily increased in size over time. This maximum surfactant/fuel ratio is higher than the ratio obtained using ATP as the chemical fuel and suggests that a higher ratio of surfactant/chemical fuel is present in these aggregates formed with DPGA. This is consistent with the data obtained by the fluorescence studies in Figure 5c.

Finally, the same experiment was performed using triphosphate as the chemical trigger. As expected, poor DLS data was collected at low concentrations of triphosphate (surfactant/triphosphate = 9:1 to 6:1), with readings of 20 ± 4 nm and 31 ± 11 nm, respectively at these two ratios. A very narrow window was observed for stable aggregate formation, attainable only at surfactant/triphosphate ratios of around 5.6:1 down to 5:1, where readings of 36 ± 10 and 50 ± 15 nm, respectively, were observed. The formation of much larger aggregates was induced at a surfactant/fuel ratio of 4.5:1, much earlier than for the previous two investigated fuels. This is again in agreement

These are not the final page numbers! ↗↗

with the data obtained from the fluorescence studies reported in Figure 5 c.

These initial investigations into the composition of the self-assembled vesicles allowed us to appreciate the complexity of systems where self-assembly is controlled by diverse chemical fuels. Not only does the composition of the supramolecular structures change, but different structures are also formed at different surfactant/trigger ratios. Fortunately, we were able to find a concentration window where it would be possible to utilise all these fuels under the same experimental conditions (Figure 6). We chose a surfactant/chemical fuel ratio of 5:1, where similar sized vesicular structures would be formed for all three chemical fuels of interest. To confirm the stability of the structures formed under these conditions, solutions of $C_{16}TACN \cdot Zn^{2+}$ (25 μM) in the presence of DPGA (5 μM) or triphosphate (5 μM) were made and found to be stable over 16 h–the formation of large aggregates and precipitation were not detected using DLS measurements. The formation of spherical aggregates with diameters in the order of 40–70 nm could also be confirmed by TEM measurements (Figure 5 e). In the absence of chemical triggers, these large sized structures could not be observed using DLS or TEM measurements.

Importantly, the DLS measurements demonstrate that the size, size distribution and stability of the aggregates critically depends on the surfactant/fuel ratio. This indicates that control over the lifetime of the assembly cannot be achieved by simply changing the concentration of the fuel employed (the addition of high concentrations of fuel will induce the formation of large, unstable aggregates), such as was possible for the nanoparticle system described earlier. From this perspec-

tive, the ability to use structural diversity as a mechanism to regulate the lifetime of the aggregates gains significantly in importance.

The behaviour of this system in the presence of different chemical fuels was next examined under dissipative conditions. The lifetime of the supramolecular structures was coupled again to the substrate specificity of the enzyme alkaline phosphatase. Thus, each of the fuels ATP, DPGA, or triphosphate (all at 5 μM) were added to a solution containing $C_{16}TACN \cdot Zn^{2+}$ (25 μM), the fluorescent probe DPH (2.5 μM), and the enzyme alkaline phosphatase (5 U m$^-$) in aqueous buffer (HEPES, 5 mM) at pH 7. At this surfactant/fuel ratio (5:1), DLS measurements had shown the formation of stable, narrowly-sized aggregates with similar dimensions. The addition of fuel caused in all cases an immediate increase in fluorescence intensity, indicative of aggregate formation (Figure 7a). For ATP, the fluorescence intensity continued to increase for 5 minutes following addition, and then steadily decreased as the concentration of ATP diminished. We were pleased to observe that also DPGA and triphosphate produced similar transient fluorescence signals. Critically, much different lifetimes of the aggregates were observed for the three compounds, which is in line with the results obtained in the transient signal generation studies. Using DPGA as the chemical fuel caused the formation of short-lived aggregates (31 minutes to reach the arbitrary end point of 50 a.u.). The aggregates induced by the addition of ATP lasted around an order of magnitude longer than the enzyme (260 minutes to reach the same end point). Finally, the structures formed by triphosphate were depleted another order of magnitude slower, this time persisting for 2800 minutes.
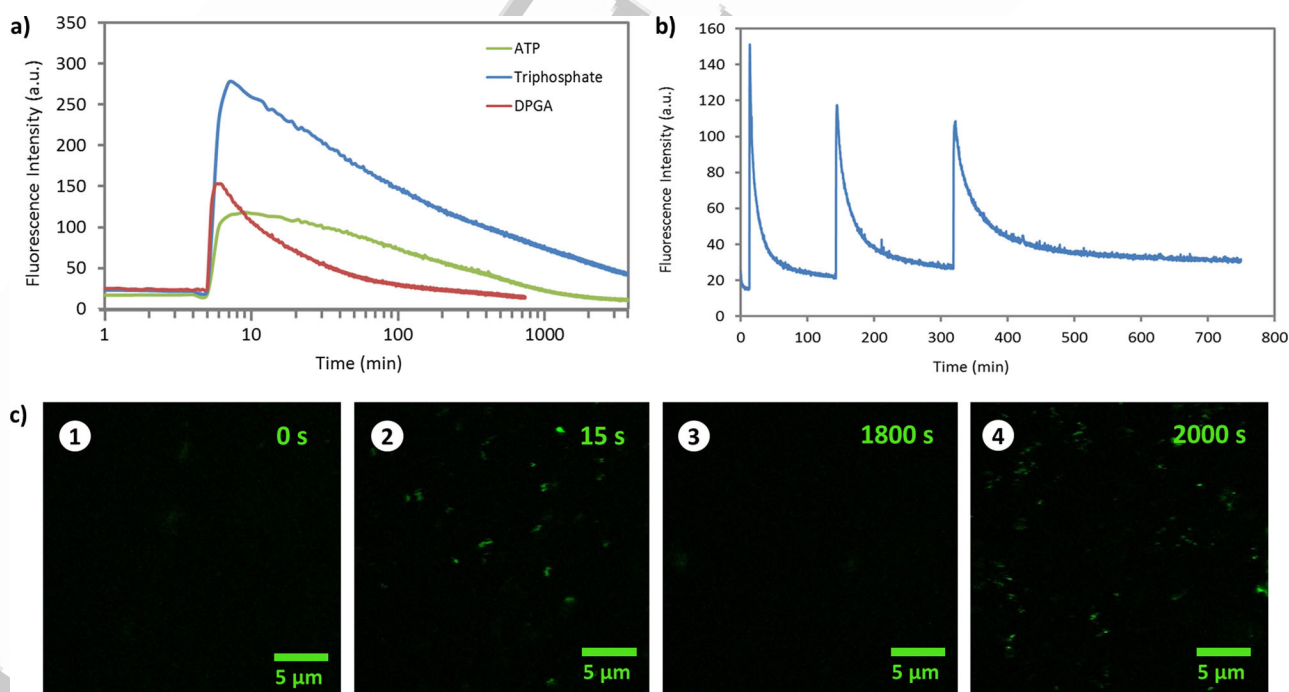

Figure 7. a) Fluorescence intensity (FI) at 428 nm as a function of time following the addition of different chemical fuels (5 μM) to $C_{16}TACN \cdot Zn^{2+}$ (25 μM) and DPH (2.5 μM) in the presence of alkaline phosphatase (5 U m$^-$) in HEPES (5 mM, pH 7.0). b) FI at 428 nm following three repetitive additions of DPGA (5 μM) to a solution of $C_{16}TACN \cdot Zn^{2+}$ (25 μM) and DPH (2.5 μM) in the presence of alkaline phosphatase (5 U m$^-$). c) Confocal images over time, showing the appearance and disappearance of fluorophore-bound vesicles in two cycles of DPGA-fuelled vesicle formation and degradation. Experimental conditions: [$C_{16}TACN \cdot Zn^{2+}$] = 25 μM, [C153] = 1 μM, [alkaline phosphatase] = 5 U m$^-$, [HEPES] = 5 mM, pH 7.0, λ_{ex} = 400 nm, λ_{em} > 510 nm.

⭇⭇ These are not the final page numbers!

The transient nature of the process was demonstrated by performing three cycles upon the repeated addition of DPGA (Figure 7b). The efficiency of DPGA in re-inducing aggregate formation reduced slightly with each cycle as a result of the accumulation of waste products. This cycling of aggregate formation could also be visually observed using laser scanning confocal microscopy studies (Figure 7c). Although the size of the aggregates is below the limit of detection of confocal microscopy, the accumulation of the hydrophobic Coumarin 152 (C153) fluorophore within the apolar part of the vesicles allowed these aggregates to be detected. Two cycles of vesicle formation and dissociation were directly visualised by recording an image every 3 seconds. Fluorescent objects appeared 10–15 seconds after the addition of each batch of DPGA, after which they decreased in number. In the absence of a chemical fuel, distinguishable fluorescent structures were not observed.

Conclusion

We have shown that temporal control over self-assembled dissipative systems can be achieved by structurally diverse chemical fuels. This was realised by coupling the transient lifetime of two different systems to the chemical structure of the fuels by using an enzyme with broad substrate specificity. It was shown that the lifetime of a fluorescent signal generated by the transient dissociation of a nanoparticle/fluorophore complex could be controlled over two orders of magnitude. The ability to control the lifetime of a transient process using different chemical fuels was found to be essential for regulating the self-assembly of vesicles. It was found that stable structures are only formed for a restricted ratio of fuels and surfactants, implying that in this case the lifetime of the structure cannot simply be changed by changing the fuel concentration. The availability of general methodology for controlling dissipative processes is an important step for the development of the next generation of adaptive, intelligent systems. The fact that this methodology can be applied for two different system shows both its robustness and flexibility. These are essential features for the construction of novel systems and networks that approach the functional complexity of natural systems.

Experimental Section

General

All commercially available reagents were used as received. 4-(2-Hydroxyethyl)-1-piperazineethanesulfonic acid (HEPES), fluorophore 1,6-diphenyl-1,3,5-hexatriene (DPH), ATP and 2,3-diphospho-D-glyceric acid penta(cyclohexalammonium) salt (DPGA) were procured from Sigma–Aldrich; 2′-deoxy-3′-O-(N′-methylanthraniloyl)adenosine-5′-O-triphos-phate (MANT-dATP) and 2′-deoxy-3′-O-(N′-methyl-anthraniloyl)adenosine-5′-O-diphosphate (MANT-dADP) were procured from Biolog Life Science Institute GmbH; and Fmoc-Ser(PO$_3$H$_2$)-OH was procured from Bachem. AuNP **1**,[21] surfactant C$_{16}$TACN[15a] and fluorescent probe C343GDD[33] were synthesised as previously described. All the above compounds were used as solutions made with mQ water. Alkaline phosphatase from bovine intestinal mucosa (P6774 Sigma) was procured from Sigma–Aldrich

and stored as a 1 kU m$^-$ solution containing 10 mM Tris buffer at pH 7.0, 5 mM MgCl$_2$ and 0.1 mM ZnCl$_2$ at 4 °C.

Instrumentation

Fluorescence measurements were performed on a Varian Cary Eclipse fluorescence spectrophotometer equipped with a thermostatted cell holder. TEM images were recorded on a Jeol 300 PX electron microscope. Dynamic light scattering measurements were recorded on a Zetasizer Nano-S (Malvern, Worcestershire, UK) equipped with a thermostatted cell holder and an Ar Laser operating at 633 nm. Confocal images were taken using a laser scanning confocal microscope (BX51WI-FV300-Olympus) coupled to a frequency doubled Ti:Sapphire femtosecond laser at 400 nm, 76 MHz (VerdiV5- Mira900-F Coherent). The laser beam was scanned on a 40×40 μm sample area with a 512×512 resolution, using a 60x water immersion objective (UPLSAPO60xW-Olympus).

Experimental Protocols

Nanoparticle concentration is expressed as a concentration of the TACN head groups on the surface of the gold nanoparticles.[34]

Determination of surface saturation concentration (SSC)

The SSC of fluorescent probe C343GDD on Au NP **1** was determined from a fluorescence titration of probe C343GDD to Au NP **1** (10 mM). The FI at 493 nm was measured as a function of the amount of C343GDD added.[21] Fitting of the experimental data yielded a SSC of 3.7±0.1 μM. For the experiments in Figures 3 and 4, sub-saturation concentrations (3.0 μM) of fluorescent probe are used to reduce background fluorescence. Experimental conditions: [TACN·Zn^{2+}] = 10±1 μM, [HEPES] = 10 mM, pH 7.0, $T = 37$ °C, $\lambda_{ex} = 450$ nm, $\lambda_{em} = 493$ nm (slits 2.5/5.0 nm).

Displacement studies

The relative affinities of the chemical probes ATP, DPGA, triphosphate, FmocPSer, dADPmant and dADPmant for the surface of Au NP **1** were determined from a series of competition experiments.[33] The displacement studies were performed by measuring the FI at 493 nm upon the addition of increasing amounts of either one of the chemical fuels to a solution of Au NP **1** (10 μM) and the fluorescent probe C343GDD (3.0 μM).

Signal dissipation

To investigate the rate at which each of the chemical fuels would be dephosphorylated by alkaline phosphatase, each chemical fuel (10 μM) was added to a pre-equilibrated solution containing Au NP **1** (10±1 μM), the fluorescent probe C343GDD (3.0 μM) and alkaline phosphatase (1U m$^-$). The chemical fuel was added at $t = 5$ min and the fluorescence intensity at $\lambda_{em} = 493$ nm (with $\lambda_{ex} = 450$ nm) was measured for the lifetime of the signal.

Transient signal generation

To demonstrate the ability of the system to sequentially respond to additional stimuli, the chemical fuels DPGA (10 μM) and ATP (8 μM) were added at the specified intervals to a pre-equilibrated solution containing Au NP **1** (10±1 μM), the fluorescent probe C343GDD (3.0 μM) and alkaline phosphatase (5 U m$^-$).

These are not the final page numbers! ↗↗

Fluorescence spectroscopy for aggregate formation

The fluorometric determination of the CAC involves the use of the hydrophobic probe DPH, which shows an increase in fluorescence intensity at concentrations higher than the CAC due to the formation of aggregates with an hydrophobic environment in which the hydrophobic fluorophore is solubilized.[15a] DPH was initially dissolved in THF to obtain a 1 mM stock solution. A 2.5 µL aliquot of this stock solution was added to a 1 mL cuvette containing aqueous HEPES buffer (5 mM, pH 7.0) to obtain a final DPH concentration of 2.5 µM. The fluorescence intensities after subsequent additions of the surfactant ($C_{16}TACN \cdot Zn^{2+}$) were recorded after the signal had stabilized (3–5 min), at $\lambda_{ex} = 355$ nm and $\lambda_{em} = 428$ nm. The temperature was maintained at 37 °C. A CAC of 106 µM was determined by extrapolation of the last four points of the curve to a fluorescence intensity of zero.[15a]

Dynamic light scattering measurements

The hydrodynamic diameter of the aggregates formed by $C_{16}TACN \cdot Zn^{2+}$ (200 µM, above the CMC) was measured in the absence of chemical fuels and in the presence of different chemical fuels (Figure 5 d). DLS experiments were also performed at different surfactant/chemical fuel ratios to understand the different supramolecular structures formed under these different conditions (Figure 6). These experiments were conducted with the Zetasizer Nano in automatic mode, where the attenuator value is adjusted by the instrument depending on sample concentration. The attenuator value is an indication of the laser power the instrument is using and varies from 1–11 with 11 signifying the highest laser power. Samples that are low in concentration or very small in size do not scatter much light, and the machine automatically increases the attenuator value to allow more light through to the sample. A high attenuator value is thus indicative of low concentrations of aggregates in the above discussion. The dispersity index is a measure of the broadness of the size distribution of the particles measured in solution. With the Zetasizer, low values indicate samples which are closer to being uniform, while higher values indicate non-uniformity (polydispersity.

TEM imaging

Samples for TEM imaging were prepared by premixing $C_{16}TACN \cdot Zn^{2+}$ (25 µM) and the chemical fuel of interest (5 µM) in HEPES pH 7 buffer (5 mM). These samples were equilibrated for 1 hour before imaging, and the samples were prepared by staining with 2% uranyl acetate solution for 30 seconds.

Fluorescence confocal microscopy studies

Fluorescence confocal images were collected of an aqueous buffered solution containing $C_{16}TACN \cdot Zn^{2+}$ (25 µM) and alkaline phosphatase (5 U m⁻), in the presence of Coumarin 153 (C153, an apolar fluorophore; 1 µM).[14a] The sample was kept inside a perfusion chamber at room temperature and after 1 minute a solution containing DPGA (final concentration of 5 µM) was rapidly injected into the chamber by a Hamilton syringe. The dynamics of vesicle formation and degradation was followed by collecting a time-series of images at the confocal microscope with temporal intervals of 3 s.

[1] a) B. A. Grzybowski, W. T. S. Huck, *Nat. Nanotechnol.* **2016**, *11*, 584–591; b) R. Merindol, A. Walther, *Chem. Soc. Rev.* **2017**, https://doi.org/10.1039/c1036cs00738d; c) Y. F. Tu, F. Peng, A. Adawy, Y. J. Men, L. K. E. A. Abdelmohsen, D. A. Wilson, *Chem. Rev.* **2016**, *116*, 2023–2078; d) J. S. Mohammed, W. L. Murphy, *Adv. Mater.* **2009**, *21*, 2361–2374; e) E. Karsenti, *Nat. Rev. Mol. Cell. Biol.* **2008**, *9*, 255–262; f) G. M. Whitesides, B. Grzybowski, *Science* **2002**, *295*, 2418–2421.

[2] a) F. della Sala, S. Neri, S. Maiti, J. L.-Y. Chen, L. J. Prins, *Curr. Opin. Biotechnol.* **2017**, *46*, 27–33; b) I. R. Epstein, B. Xu, *Nat. Nanotechnol.* **2016**, *11*, 312–319; c) E. Mattia, S. Otto, *Nat. Nanotechnol.* **2015**, *10*, 111–119; d) T. Le Saux, R. Plasson, L. Jullien, *Chem. Commun.* **2014**, *50*, 6189–6195; e) D. K. Kumar, J. W. Steed, *Chem. Soc. Rev.* **2014**, *43*, 2080–2088; f) S. C. Warren, O. Guney-Altay, B. A. Grzybowski, *J. Phys. Chem. Lett.* **2012**, *3*, 2103–2111; g) S. Mann, *Nat. Mater.* **2009**, *8*, 781–792.

[3] M. Fialkowski, K. J. M. Bishop, R. Klajn, S. K. Smoukov, C. J. Campbell, B. A. Grzybowski, *J. Phys. Chem. B* **2006**, *110*, 2482–2496.

[4] B. A. Grzybowski, C. E. Wilmer, J. Kim, K. P. Browne, K. J. M. Bishop, *Soft Matter* **2009**, *5*, 1110–1128.

[5] For *general reviews*, see: a) W. Lu, X. Le, J. Zhang, Y. Huang, T. Chen, *Chem. Soc. Rev.* **2017**, *46*, 1284–1294; b) P. A. Gale, J. W. Steed, *Supramolecular Chemistry: From Molecules to Nanomaterials*, Wiley, **2012**; for magnetisation as trigger, see: c) B. A. Grzybowski, H. A. Stone, G. M. Whitesides, *Nature* **2000**, *405*, 1033–1036; for *light* as a trigger, see: d) H. Zhao, S. Sen, T. Udayabhaskararao, M. Sawczyk, K. Kucanda, D. Manna, P. K. Kundu, J. W. Lee, P. Kral, R. Klajn, *Nat. Nanotechnol.* **2016**, *11*, 82–88; e) S. Ito, H. Yamauchi, M. Tamura, S. Hidaka, H. Hattori, T. Hamada, K. Nishida, S. Tokonami, T. Itoh, H. Miyasaka, T. Iida, *Sci. Rep.* **2013**, *3*, 3047; f) R. Klajn, K. J. M. Bishop, B. A. Grzybowski, *Proc. Natl. Acad. Sci. USA* **2007**, *104*, 10305–10309; for redox energy as a trigger, see: g) C. Y. Cheng, P. R. McGonigal, S. T. Schneebeli, H. Li, N. A. Vermeulen, C. F. Ke, J. F. Stoddart, *Nat. Nanotechnol.* **2015**, *10*, 547–553; h) S. O. Krabbenborg, J. Veerbeek, J. Huskens, *Chem. Eur. J.* **2015**, *21*, 9638–9644; i) C. Y. Cheng, P. R. McGonigal, W. G. Liu, H. Li, N. A. Vermeulen, C. F. Ke, M. Frasconi, C. L. Stern, W. A. Goddard, J. F. Stoddart, *J. Am. Chem. Soc.* **2014**, *136*, 14702–14705; for osmotic pressure as a trigger, see: j) R. S. M. Rikken, R. Engelkamp, R. J. M. Nolte, J. C. Maan, J. C. M. van Hest, D. A. Wilson, P. C. M. Christianen, *Nat. Commun.* **2016**, *7*, 12606; for chemical fuels as trigger, see: k) B. S. L. Collins, J. C. M. Kistemaker, E. Otten, B. L. Feringa, *Nat. Chem.* **2016**, *8*, 860–866; l) M. R. Wilson, J. Sola, A. Carlone, S. M. Goldup, N. Lebrasseur, D. A. Leigh, *Nature* **2016**, *534*, 235–241; m) S. P. Fletcher, F. Dumur, M. M. Pollard, B. L. Feringa, *Science* **2005**, *310*, 80–82.

[6] For examples using light as a trigger: a) P. K. Kundu, D. Samanta, R. Leizrowice, B. Margulis, H. Zhao, M. Borner, T. Udayabhaskararao, D. Manna, R. Klajn, *Nat. Chem.* **2015**, *7*, 646–652; b) G. Ragazzon, M. Baroncini, S. Silvi, M. Venturi, A. Credi, *Nat. Nanotechnol.* **2015**, *10*, 70–75; c) R. Klajn, P. J. Wesson, K. J. M. Bishop, B. A. Grzybowski, *Angew. Chem. Int. Ed.* **2009**, *48*, 7035–7039; *Angew. Chem.* **2009**, *121*, 7169–7173; d) T. Soejima, M. Morikawa, N. Kimizuka, *Small* **2009**, *5*, 2043–2047; e) C. G. Pappas, T. Mutasa, P. W. J. M. Frederix, S. Fleming, S. Bai, S. Debnath, S. M. Kelly, A. Gachagan, R. V. Ulijn, *Mater. Horiz.* **2015**, *2*, 198–202; using pH changes as a trigger: f) T. Heuser, A. K. Steppert, C. M. Lopez, B. L. Zhu, A. Walther, *Nano Lett.* **2015**, *15*, 2213–2219; an example of an

oscillatory system: g) T. Ikegami, Y. Kageyama, K. Obara, S. Takeda, *Angew. Chem. Int. Ed.* **2016**, *55*, 8239–8243; *Angew. Chem.* **2016**, *128*, 8379–8383; an example of an out-of-equilibrium system: h) J. Palacci, S. Sacanna, A. P. Steinberg, D. J. Pine, P. M. Chaikin, *Science* **2013**, *339*, 936–940.

[7] T. Aida, E. W. Meijer, S. I. Stupp, *Science* **2012**, *335*, 813–817.

[8] M. A. C. Stuart, W. T. S. Huck, J. Genzer, M. Muller, C. Ober, M. Stamm, G. B. Sukhorukov, I. Szleifer, V. V. Tsukruk, M. Urban, F. Winnik, S. Zauscher, I. Luzinov, S. Minko, *Nat. Mater.* **2010**, *9*, 101–113.

[9] For a general review, see: E. Busseron, Y. Ruff, E. Moulin, N. Giuseppone, *Nanoscale* **2013**, *5*, 7098–7140.

[10] K. Kitamura, M. Tokunaga, A. H. Iwane, T. Yanagida, *Nature* **1999**, *397*, 129–134.

[11] a) A. J. M. Wollman, C. Sanchez-Cano, H. M. J. Carstairs, R. A. Cross, A. J. Turberfield, *Nat. Nanotechnol.* **2014**, *9*, 44–47; b) C. Hoffmann, E. Mazari, S. Lallet, R. Le Borgne, V. Marchi, C. Gosse, Z. Gueroui, *Nat. Nanotechnol.* **2013**, *8*, 199–205; c) T. Sanchez, D. T. N. Chen, S. J. DeCamp, M. Heymann, Z. Dogic, *Nature* **2012**, *491*, 431–435; d) H. Q. Liu, E. D. Spoerke, M. Bachand, S. J. Koch, B. C. Bunker, G. D. Bachand, *Adv. Mater.* **2008**, *20*, 4476–4481; e) H. Hess, J. Clemmens, C. Brunner, R. Doot, S. Luna, K. H. Ernst, V. Vogel, *Nano Lett.* **2005**, *5*, 629–633; f) A. Kakugo, S. Sugimoto, J. P. Gong, Y. Osada, *Adv. Mater.* **2002**, *14*, 1124–1126.

[12] a) G. T. Wang, B. H. Tang, Y. Liu, Q. Y. Gao, Z. Q. Wang, X. Zhang, *Chem. Sci.* **2016**, *7*, 1151–1155; b) I. Lagzi, B. Kowalczyk, D. W. Wang, B. A. Grzybowski, *Angew. Chem. Int. Ed.* **2010**, *49*, 8616–8619; *Angew. Chem.* **2010**, *122*, 8798–8801; c) S. Maeda, Y. Hara, R. Yoshida, S. Hashimoto, *Angew. Chem. Int. Ed.* **2008**, *47*, 6690–6693; *Angew. Chem.* **2008**, *120*, 6792–6795; d) S. Shinohara, T. Seki, T. Sakai, R. Yoshida, Y. Takeoka, *Angew. Chem. Int. Ed.* **2008**, *47*, 9039–9043; *Angew. Chem.* **2008**, *120*, 9179–9183; e) S. Maeda, Y. Hara, T. Sakai, R. Yoshida, S. Hashimoto, *Adv. Mater.* **2007**, *19*, 3480–3484; f) V. V. Yashin, A. C. Balazs, *Science* **2006**, *314*, 798–801.

[13] For an example of an exception, see: S. N. Semenov, A. S. Y. Wong, R. M. van der Made, S. G. J. Postma, J. Groen, H. W. H. van Roekel, T. F. A. de Greef, W. T. S. Huck, *Nat. Chem.* **2015**, *7*, 160–165.

[14] a) S. Dhiman, A. Jain, S. J. George, *Angew. Chem. Int. Ed.* **2017**, *56*, 1329–1333; *Angew. Chem.* **2017**, *129*, 1349–1353; b) C. A. Angulo-Pachon, J. F. Miravet, *Chem. Commun.* **2016**, *52*, 5398–5401; c) J. Boekhoven, W. E. Hendriksen, G. J. M. Koper, R. Eelkema, J. H. van Esch, *Science* **2015**, *349*, 1075–1079; d) C. G. Pappas, I. R. Sasselli, R. V. Ulijn, *Angew. Chem. Int. Ed.* **2015**, *54*, 8119–8123; *Angew. Chem.* **2015**, *127*, 8237–8241; e) M. Kumar, P. Brocorens, C. Tonnele, D. Beljonne, M. Surin, S. J. George, *Nat. Commun.* **2014**, *5*, 5793; f) S. Debnath, S. Roy, R. V. Ulijn, *J. Am. Chem. Soc.* **2013**, *135*, 16789–16792; g) M. Kumar, N. Jonnalagadda, S. J. George, *Chem. Commun.* **2012**, *48*, 10948–10950; h) J. Boekhoven, A. M. Brizard, K. N. K. Kowlgi, G. J. M. Koper, R. Eelkema, J. H. van Esch, *Angew. Chem. Int. Ed.* **2010**, *49*, 4825–4828; *Angew. Chem.* **2010**, *122*, 4935–4938.

[15] a) S. Maiti, I. Fortunati, C. Ferrante, P. Scrimin, L. J. Prins, *Nat. Chem.* **2016**, *8*, 725–731; b) A. K. Dambenieks, P. H. Q. Vu, T. M. Fyles, *Chem. Sci.* **2014**, *5*, 3396–3403.

[16] a) C. S. Wood, C. Browne, D. M. Wood, J. R. Nitschke, *ACS Cent. Sci.* **2015**, *1*, 504–509; For an example where the assembly itself catalyses the depletion of the fuel, see: b) H. Fanlo-Virgós, A. N. R. Alba, S. Hamieh, M. Colomb-Delsuc, S. Otto, *Angew. Chem. Int. Ed.* **2014**, *53*, 11346–11350; *Angew. Chem.* **2014**, *126*, 11528–11532.

[17] C. Pezzato, L. J. Prins, *Nat. Commun.* **2015**, *6*, 7790.

[18] G. M. Whitesides, R. F. Ismagilov, *Science* **1999**, *284*, 89–92.

[19] B. Alberts, A. Johnson, J. Lewis, D. Morgan, M. Raff, K. Roberts, P. Walter, *Molecular Biology of the Cell, Sixth Edition*, Garland Science New York, 6th edn. **2015**.

[20] a) J. S. Wu, W. M. Liu, J. C. Ge, H. Y. Zhang, P. F. Wang, *Chem. Soc. Rev.* **2011**, *40*, 3483–3495; b) E. V. Anslyn, *J. Org. Chem.* **2007**, *72*, 687–699; c) C. W. Rogers, M. O. Wolf, *Coord. Chem. Rev.* **2002**, *233*, 341–350; d) P. D. Beer, P. A. Gale, *Angew. Chem. Int. Ed.* **2001**, *40*, 486–516; *Angew. Chem.* **2001**, *113*, 502–532; e) B. Valeur, I. Leray, *Coord. Chem. Rev.* **2000**, *205*, 3–40.

[21] G. Pieters, A. Cazzolaro, R. Bonomi, L. J. Prins, *Chem. Commun.* **2012**, *48*, 1916–1918.

[22] a) G. Pieters, C. Pezzato, L. J. Prins, *Langmuir* **2013**, *29*, 7180–7185; b) R. Bonomi, A. Cazzolaro, A. Sansone, P. Scrimin, L. J. Prins, *Angew. Chem. Int. Ed.* **2011**, *50*, 2307–2312; *Angew. Chem.* **2011**, *123*, 2355–2360.

[23] a) K. Saha, S. S. Agasti, C. Kim, X. N. Li, V. M. Rotello, *Chem. Rev.* **2012**, *112*, 2739–2779; b) U. H. F. Bunz, V. M. Rotello, *Angew. Chem. Int. Ed.* **2010**, *49*, 3268–3279; *Angew. Chem.* **2010**, *122*, 3338–3350.

[24] a) C. Cekic, J. Linden, *Nat. Rev. Immunol.* **2016**, *16*, 177–192; b) G. Burnstock, *Nat. Rev. Drug. Discovery* **2008**, *7*, 575–590.

[25] J. Molnar, L. Lorand, *Arch. Biochem. Biophys.* **1961**, *93*, 353–363.

[26] D. Barford, A. K. Das, M. P. Egloff, *Annu. Rev. Biophys. Biomol. Struct.* **1998**, *27*, 133–164.

[27] C. Pezzato, P. Scrimin, L. J. Prins, *Angew. Chem. Int. Ed.* **2014**, *53*, 2104–2109; *Angew. Chem.* **2014**, *126*, 2136–2141.

[28] J. E. Coleman, *Annu. Rev. Biophys. Biomol. Struct.* **1992**, *21*, 441–483.

[29] A. Desai, T. J. Mitchison, *Annu. Rev. Cell Dev. Biol.* **1997**, *13*, 83–117.

[30] P. Walde, H. Umakoshi, P. Stano, F. Mavelli, *Chem. Commun.* **2014**, *50*, 10177–10197.

[31] a) G. C. Li, S. Y. Zhang, N. J. Wu, Y. Y. Cheng, J. S. You, *Adv. Funct. Mater.* **2014**, *24*, 6204–6209; b) Z. Kostereli, K. Severin, *Chem. Commun.* **2012**, *48*, 5841–5843; c) R. Sasaki, S. Murata, *Langmuir* **2008**, *24*, 2387–2394.

[32] I. Cruz-Campa, A. Arzola, L. Santiago, J. G. Parsons, A. Varela-Ramirez, R. J. Aguilera, J. C. Noveron, *Chem. Commun.* **2007**, 2944–2946.

[33] C. Pezzato, B. Lee, K. Severin, L. J. Prins, *Chem. Commun.* **2013**, *49*, 469–471.

[34] A. Scarso, G. Zaupa, F. B. Houillon, L. J. Prins, P. Scrimin, *J. Org. Chem.* **2007**, *72*, 376–385.

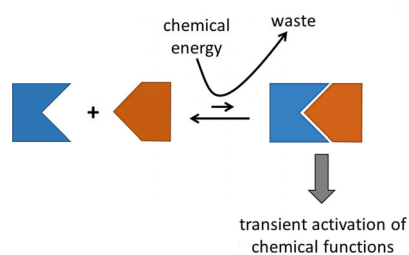**These are not the final page numbers!** ↗↗

FULL PAPER

■ Systems Chemistry

J. L.-Y. Chen, S. Maiti, I. Fortunati,
C. Ferrante, L. J. Prins*

■■ – ■■

Temporal Control over Transient
Chemical Systems using Structurally
Diverse Chemical Fuels

chemical energy → waste

transient activation of chemical functions

Chemical fuels to control lifetime: The next generation of adaptive, intelligent materials will require precise control over energy dissipation processes. Towards this goal, structurally diverse chemical fuels are used to control the lifetime of two such processes: transient signal generation and transient self-assembly.

#HotPaper #chemistry on chemical fuels for controlling intelligent systems @UniPadova SPACE RESERVED FOR IMAGE AND LINK

Share your work on social media! *Chemistry - A European Journal* has added Twitter as a means to promote your article. Twitter is an online microblogging service that enables its users to send and read text-based messages of up to 140 characters, known as "tweets". Please check the pre-written tweet in the galley proofs for accuracy. Should you or your institute have a Twitter account, please let us know the appropriate username (i.e., @accountname), and we will do our best to include this information in the tweet. This tweet will be posted to the journal's Twitter account @ChemEurJ (follow us!) upon online publication of your article, and we recommended you to repost ("retweet") it to alert other researchers about your publication.

Please check that the ORCID identifiers listed below are correct. We encourage all authors to provide an ORCID identifier for each coauthor. ORCID is a registry that provides researchers with a unique digital identifier. Some funding agencies recommend or even require the inclusion of ORCID IDs in all published articles, and authors should consult their funding agency guidelines for details. Registration is easy and free; for further information, see http://orcid.org/.

Dr. Jack L.-Y. Chen
Dr. Subhabrata Maiti
Dr. Ilaria Fortunati
Prof. Dr. Camilla Ferrante
Prof. Dr. Leonard J. Prins http://orcid.org/0000-0001-6664-822X

◄◄ These are not the final page numbers!